Assessment of the usefulness of image reconstruction in the oblique and double-oblique sagittal planes for magnetic resonance imaging of the canine cranial cruciate ligament

Adam Przeworski[1], Zbigniew Adamiak[2], Michał Nowicki[3],
Marta Mieszkowska[4], Angelika Tobolska[4⊠], Joanna Głodek[4]

[1]Veterinary Clinic Tworkowski Przeworscy, 10-685 Olsztyn, Poland
[2]Small Animal Clinic, 15-306 Białystok, Poland
[3]Vet4Pet Veterinary Clinic, 04-052 Warsaw, Poland
[4]Department of Surgery and Roentgenology with Clinic, Faculty of Veterinary Medicine,
University of Warmia and Mazury in Olsztyn, 10-719 Olsztyn, Poland
angelika.tobolska@uwm.edu.pl

Abstract

Introduction: The aim of the study was to determine the quality and significance of the magnetic resonance image of the canine knee after reconstruction in the oblique and double-oblique sagittal plane. This reconstruction and 3D images are rarely used in common protocols due to the longer study time they require. The study aimed to demonstrate significance for such diagnostic images in specific sequences in order to stimulate consideration of their more frequent use in diagnosis of diseases of the cruciate ligament in dogs. **Material and Methods:** All tests were carried out using an open magnetic resonance tomography scanner with magnetic field induction. The images obtained from the 30 canine patients examined were reconstructed and evaluated by independent appraisers. Statistical analysis was performed. **Results:** The study showed that MRI of the stifle joint using 3D sequences provides higher quality images of the cranial cruciate ligament in dogs. The results of the statistical analysis showed that multi-faceted reconstruction allows the secondary determination of the oblique imaging planes and obtains images of adequate quality. **Conclusion:** It can be concluded that multi-faceted reconstruction facilitates the secondary determination of oblique imaging planes. This reconstruction additionally makes images available of better quality compared to the 2D sequence.

Keywords: MRI, stifle joint, imaging, dog.

Introduction

The technique of three-dimensional signal acquisition is not widely used. Although both the two- and three-dimensional methods obtain a series of images of the tested object, in 3D sequences, the signal is additionally received in the direction of the 3D coding phase from the specified volume of the object. This means that the obtained data can be reconstructed (by Fourier transform) and the possibility is granted of changing the thickness of the layer and the imaging plane. The images obtained in 3D sequences have high tissue signal intensity, good signal-to-noise ratio (SNR), high image resolution, and fewer volume averaging artefacts. Unfortunately, the image acquisition time in 3D sequences is usually longer than in 2D sequences, which can potentially increase the risk of movement artefacts and cause the sequence to be repeated (35).

Multi-plane reconstruction (MPR) of the obtained signal in order to gain a different imaging plane was used only in two works on the canine knee joint. In both cases, they employed high-field devices (12, 13). In the case of low-field devices, MPR reconstruction was used when imaging the knee joint of a marsh deer (*Blastocerus dichotomous*) (42).

Particular interest in the possibility of image reconstruction can be observed in human medicine. Although it was mainly used in research with the application of high-field devices (16, 21, 30, 34, 35, 39, 47), its use has also been described with low-field systems in operation (31).

The low-field device image was characterised by lower spatial resolution and poorer quality, but it allowed more layers to be obtained in a given cross-section.

The suitability of MPR in diagnosis has not been conclusively proven. Notohamiprodjo et al. (30) obtained comparable SNR and (contrast-to-noise ratio) (CNR) values for layers (of equal thickness) after MPR and 2D. Lee et al. (31) obtained anterior cruciate ligament (ACL) images with higher SNR and CNR values than 2D sequences using 3D VISTA (Volume ISotropic Turbo spin echo Acquisition) sequences; unfortunately, they were less sharp, which did not affect the diagnostic possibilities, however. The use of MPR can potentially shorten the overall examination time and it made detection possible of small changes in the menisci and ligaments that were not noticeable in the 2D sequence images (47). The possibility of multi-faceted reconstruction consisting of very thin layers of the examined object without the need for gaps between them was taken advantage of image menisci in the transverse plane (31). Pass et al. (35) however, unlike previous authors, did not recommend replacing 2D sequences in three planes with images derived from MPR of 3D sequences because of deterioration in the accuracy of meniscus and cartilage damage detection.

In order to improve the visualisation of the ligament in human medicine, it is recommended to lay the knee slightly rotated to the outside, or oblique imaging planes are used. In veterinary medicine, there is little information on canine cranial cruciate ligament (CCL) imaging plane choice. Most authors defined the plane "according to the course of the CCL", usually in the sagittal plane (2, 17, 36, 37, 38, 41, 44). It was not until 2007 that Winegardner et al. (46) further described the course of knee imaging planes used, including imaging the CCL. In 2014 in a study on anatomical preparation for imaging, Podadera et al. (36) determined the angle of bend of the knee joint and the course of the imaging plane which afforded the most accurate visualisation of the CCL. Standard sagittal plane imaging was carried out parallel to the medial condyle of the femur, and sagittal oblique plane imaging was also captured based on locating sequences in the frontal and transverse plane. Despite the use of skewed imaging planes in the study being novel, their significance was not analysed in detail. Similarly to previous authors, Fazio et al. (10) planned the oblique plane of CCL imaging. They used the locating sequence in the frontal plane, running lines parallel to the lateral femoral condyle.

Most authors presented greater effectiveness of ACL imaging or finer detection of its damage using oblique planes (sagittal, frontal, transverse). However, the use of both the sagittal and oblique frontal planes in the protocol did not augment diagnostic effectiveness (20). Oblique imaging planes were also used for postoperative assessment, where additional oblique imaging planes (sagittal and frontal) increased the specificity and accuracy of graft assessment after ACL reconstructive surgery (19).

The purpose of the present study was to determine the diagnostic value of the image obtained after multi-plane reconstruction in the oblique imaging planes. This report also describes the consistency in assessment between the technicians surveying the images and the internal consistency of individual technicians. The study also determined the values of the angles of inclination of the oblique cross-sectional planes which allow the entire sacral ligament to be visualised.

Material and Methods

In the years 2014–2017, 30 mainly non-breed dogs of both sexes were assessed, aged 1.5 to 12 years (average age 5.2). The average weight of the dogs was 25.1 kg (ranging from 13.5 kg to 45 kg). There were 8 females (26.7%) and 22 males (73.3%). Most often, one joint was examined; 18 left (60%) and 12 right (40%) knee joints were inspected. If there were no contraindications, the animal was further qualified for the study based on clinical, orthopaedic and radiological examinations. In the event of suspected or established pathological changes (degenerative changes, tumours, metal implants, or fractures) in the knee joint and its surrounding area, the animal was excluded from further study.

All tests were performed using an open magnetic resonance tomograph with magnetic field induction of 0.245 T ± 5.0 mT (Vet-MR Grande, Esaote, Genova, Italy) permanent magnet, gradient strength of 20 mT/m, and gradient slew rate of 25 mT/m/s. A dedicated veterinary receiving dual-phase array knee coil with internal diameter of 14.3 × 16 × 18.3 cm was used.

Magnetic resonance imaging was performed on animals under general anaesthesia. The animals were placed in the lateral position with the examined limb on top. The knee joint was placed in the coil. Using a plastic Saehan goniometer, the angle closest to the physiological angle, i.e., the normal standing angle, was fixed. The mean knee bend angle was 139° (SD 7.1°; range: 127°–151°).

The knee imaging protocol used during the study consisted of a) a 2D spin-echo sequence of T1-dependent images obtained in three planes: sagittal, frontal, and transverse and b) a 3 D spin-echo sequence of T1-dependent images obtained in the sagittal plane. The detailed parameters of the imaging protocol used are presented in Table 1.

In the sagittal plane, the course of the layers was determined thus: in the transverse image it was perpendicular to the tangent line to the caudal edge of the femoral condyle and in the frontal image perpendicular to the tibial plateau. In the frontal plane, the course of the layers was determined thus: in the transverse image it was tangential to the caudal edge of the femoral condyle, and in the sagittal image parallel to the patellar ligament. Lastly, in the transverse plane, the course of the layers was determined thus: in the frontal

image it was parallel to the tibial plateau and tangential to the femoral condyles, and on the sagittal image perpendicular to the straight patellar ligament.

Data obtained with isotropic 3D sequences were used for MPR. It was performed after the test using dedicated software (Opi, release 1.2B E-MRI Brio BUILD_20 SP1, Esaote).

The section plane was determined during geometric planning using images obtained in the 3D scout process. During preparation, the function of previewing the obtained cross-section in real-time was helpful and minimised the need to use localising sequences (localiser or topogram).

Then oblique cross-sectional planes were determined to be diagonal sagittal and double-sagittal.

In the first in the frontal image, the imaging plane was tilted according to the anatomical course of the CCL. On the transverse image, the plane was determined perpendicular to the tangent line to the caudal edge of the femoral condyle. The double-oblique sagittal plane was determined in two stages: in the first one, the oblique course was determined on the transverse image, then in the second, the oblique course was determined on the frontal images. The imaging plane was set until the best ligament visibility was achieved based on the subjective visual assessment of the person performing the procedure. In all cases it was the same person.

The detailed parameters of the sequences used are shown in Table 2.

Table 1. Parameters of 2D and 3D spin-echo sequences of T1-dependent images used during the study

Sequence	T1 Spin Echo HF	Spin Echo T1 3D HF
Echo time (TE, ms)	18 (15–30)	24
Repetition time (TR, ms)	950 (750–1150)	300
Number of signal averages (NEX)	1	1
Image field size (FOV, mm × mm)	200 × 200 (200–220 × 180–200)	150 × 150 (150–200 × 130–200)
3D image field size (FOV 3D)	nd	70 (50–90)
Imaging matrix (mm × mm)	192 × 115 (192–256 × 115–216)	192 × 152 (192–256 × 132– 200)
Layer thickness (mm)	3	1.9
Spacing between layers (mm)	0.3	0
Number of images (most common, range)	18 (15–30)	26 (26–52)

nd – not detected

Table 2. Parameters of T1-dependent images after multi-plane reconstruction (MPR) used during the study

Sequence	MPR
Echo time (TE, ms)	24
Repetition time (TR, ms)	300
Number of signal averages (NEX)	1
Image field size (FOV, mm × mm)	150 × 150 (150–200 × 150–200)
3D image field size (FOV 3D)	N/A
Imaging matrix (mm × mm)	256 × 152 (196–256 × 150–168)
3D imaging matrix	N/A
Layer thickness (mm)	0.6
Spacing between layers (mm)	0
Number of images (most common, range)	65 (23–87)

N/A – not applicable
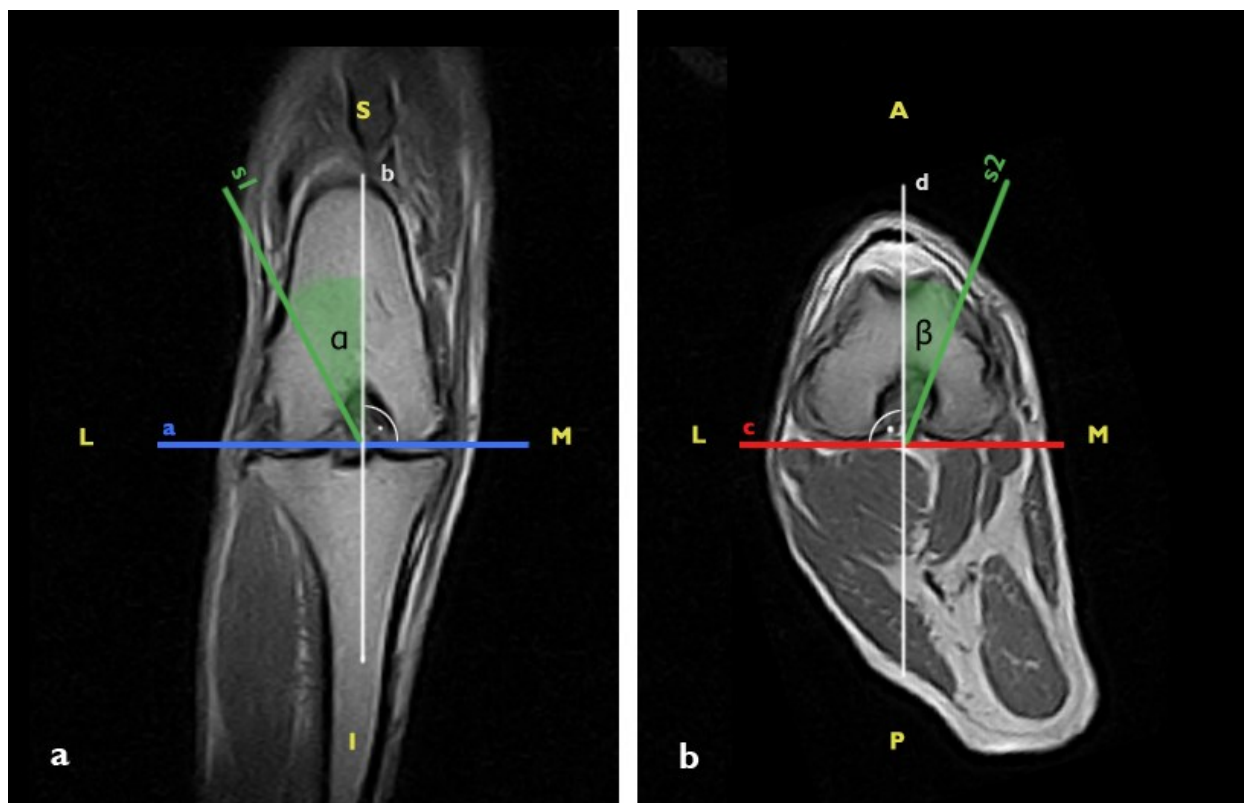
Fig. 1. The method of determining the values of the inclination angles of the inclined sagittal (α) and double-oblique (α, β) planes on the images in the frontal (a) and transverse (b) planes. Auxiliary lines: a, b, c, d, s1, s2 (A – anterior; I – inferior; L – lateral; M – medial; P – posterior; S – superior)

In the next stage of the study, the angle of inclination of the plane relative to the classical course of the imaging plane was determined. Angles were measured by a person who had previously performed a multi-plane reconstruction. When determining the angle value, images obtained in the frontal and transverse planes were used. To determine the angle of inclination of the oblique section planes, a reference line (available in the software options and showing the course of the layers in space) and auxiliary lines (a, b, c, d, s1, s2) were added to the images. Proper angles of inclination are marked as α and β.

In the frontal images, a line (a) parallel to the articular surface of the tibial plateau and tangential to the lateral and medial femoral condyles was determined. Then two lines were determined: a perpendicular (b) to line a and a parallel to the reference line (s1). The angle of inclination (α) was the angle between line b and line s1 (Fig. 1a).

In the case of double-skewed planes, the angle β was additionally determined based on images in the transverse plane. First, a line (c) was added tangentially to the caudal edges of the femoral condyles, then a line (d) perpendicular to line c was drawn. Finally, a line parallel to the reference line (s2) was drawn. The angle between line d and line s2 was the slope of the oblique section plane (Fig. 1b).

The statistical analysis was made using the Statistica v.12.5 program (StatSoft, Tulsa, OK, USA).

The Mann–Whitney U test was used to test the statistical significance of differences. A P value of ≤ 0.05 meant that a difference between values was statistically significant.

Results

The data were anonymised before the evaluation. The obtained series of images were evaluated randomly and independently by three MRI technicians. The evaluation was carried out according to the prepared protocol twice with an interval of three weeks. To make certain of objective interpretation, the evaluators did not know the details of the study.

First, the images were subjected to visual assessment, during which attention was paid to the image sharpness, blur, contrast between soft tissues, noise, and presence of artefacts or distortions. Image quality was assessed based on a five-degree ordinal scale according to Likert (22): 1) low, 2) below average, 3) medium, 4) good, or 5) high.

Next, the visibility of the cranial cruciate ligament was determined. The assessment scale was developed based on the visual assessment score presented by Podadera *et al.* (36). It was as follows for the cranial cruciate ligament: 0 – CCL invisible; 1 – CCL partially visible in the images; 2 – CCL visible in full with a blurred boundary; 3 – CCL visible in full with a clearly

defined boundary. The number of images in which the CCL was visible was also determined.

The data did not have a normal distribution and therefore nonparametric tests were selected for analysis. The statistical tests determined whether there was a statistically significant difference between the results of the assessments in individual sequences and to what extent the assessors were in agreement for individual features. The consistency of individual evaluators' scores in the two assessments separated by the three-week interval was also established. The Mann–Whitney U test was used to test the statistical significance of differences and the valid P value was as noted above. The consistency of assessments between the evaluators was determined using the Kendall compliance factor separately for each of the two assessments. Similarly, the level of accord of the individual evaluators' assessments was determined for the two evaluations. The compliance factor W assumes values between 0 (no agreement) and 1 (full agreement).

The number of images with a visible ligament obtained using MPR in the double-oblique sagittal plane was significantly higher than that in the oblique sagittal plane. In the second assessment, the same median number of layers was obtained using MPR with the oblique as with the double-oblique sagittal plane. However, the images in the double-oblique sagittal plane were characterised by a higher rank sum (Fig 1).

Magnetic resonance imaging is a useful method of visualising structures within a dog's knee joint. The standard test protocol usually consists of 2D sequences. The use of an additional 3D sequence during the test creates the possibility of multi-plane reconstruction at any time after the test (Tables 1 and 2). This allows new images to be reconstructed in any plane using previously obtained data. It is thereby possible to improve the previously defined imaging plane or to present the structure in an additional plane.

Discussion

In the available literature, the authors used different coils depending on their device and test assumptions. Most often, these were rigid or flexible organ coils dedicated to limb imaging and included elbow (37), carpal (2), knee (5, 32, 40, 43), and spinal (4) varieties, which were also solenoidal (44) or dual-phased array coils (8, 15, 46). The selection for this study of a dual-phased array knee coil allowed for better image quality due to the higher SNR. Due to the significant correlation between the weight of dogs and the quality of images from 3D sequences, it can be assumed that the differences in dog size and the closeness of fit of the coil to the knee potentially affected the quality of the study. Nemec *et al.* (26) experienced a positive effect of suitable matching of the coil diameter to the examined structure on the diagnostic quality of the obtained images.

The study described in the article was carried out in a lateral position with the examined limb up. The joint was placed in the coil in physiological flexion with some deviations related to the size of the joints. Currently, apart from the manufacturer's instructions, there are no guidelines regarding the positioning of the dog for knee imaging. In other articles, dogs were placed in the dorsal (2, 5, 12, 23, 24, 32, 40, 43, 44) lateral (4, 11, 36, 37) or bridge position (15).

Both the position of the joint in the coil and the angle of bending affect the spatial location of the cruciate ligament in relation to the magnetic field lines. Spriet *et al.* (45) determined that imaging of the ligament at an angle of $55° \pm 10°$ to the magnetic field line promotes the creation of a magic angle artefact, which increases the signal intensity of the examined structure. Most low-field systems have a vertical magnetic field orientation, which should be taken into account during resonance imaging. The current authors cannot exclude the occurrence of this phenomenon in the study, especially when using the lateral arrangement.

Image quality assessment spanned a significant range (which was identical for all sequences). The lowest-rated images were defined as below average, while the highest rated images were high. Only in the case of images from 3D sequences was the quality was rated as good and high in over 50% of captures Images obtained using 3D sequences in the sagittal plane improved CCL visibility and a significantly higher number of them presented a visible CCL compared to images using 2D sequences. Only two studies on imaging CCL damage in dogs have thoroughly analysed the diagnostic capabilities of 3D sequences (38, 41). Both teams used high-field magnetic resonance imaging with 3 T magnetic field induction. The 3D FSE (Fast Spin Echo) CUBE (GE Healthcare) sequence allowed for the assessment of partial CCL tears and proper evaluation of the severity of knee synovitis, and the VIPR-aTR (Vastly under-sampled Isotropic PRojection with alternating length repetition times) 3D sequence allowed better estimation of the structural properties of CCL assessed on anatomical models (*ex vivo* test) (41). In human medicine, 2D and 3D sequences were compared when imaging various knee structures. Most studies have shown the comparable diagnostic utility of both sequences (1, 9, 16, 18). Ristow *et al.* (39) noticed that low-contrast structures were usually rated worse than high-contrast structures.

The potential for improving the efficiency of ACL imaging using oblique planes has been carefully evaluated in human medicine. Buckwalter and Pennes (7) proposed using a template printed on transparent film to determine the sagittal plane at an angle of 15° to the classical plane. Nakanishi *et al.* (25) fixed the plane at an angle of 10° but increased this angle to 20° if they did not originally achieve satisfactory ACL visualisation. Barberie *et al.* (3) determined that planning an oblique imaging plane using the locating sequence in the frontal plane allows more accurate ACL imaging than using the

locating sequence in the transverse plane. The intact ACL spatial arrangement and the oblique sagittal, frontal and transverse imaging planes were compared by Breitenseher and Mayerhoefer (6), who achieved the best results using planes at an angle of 20° to the classical plane. Nenezić and Kocijancic (27) determined that both imaging of a bent knee joint and the use of oblique sagittal plane imaging increased the sensitivity of detection of partial tears of the ACL. No statistical difference was observed between the two techniques. Subsequent authors evaluated the possibilities of other oblique imaging planes. Thinner layers (1 mm) and the use of an oblique face increased the efficiency of ACL damage detection (14). The influence of additional sequences in the oblique planes on the overall effectiveness of ACL imaging was also assessed. It was found that the use of a combination of images obtained in the classical planes and the oblique frontal plane during the evaluation gave higher specificity in detecting ACL damage for 3 T devices than 1.5 T devices (33). Ng *et al*. (29) obtained higher imaging sensitivity (71%) of intact ACL using additional images in the oblique transverse plane. Also, the use of additional images obtained in the oblique transverse plane when this plane was in the protocol increased the sensitivity of ACL partial tear detection from 33% to 87% (27) and from 74% to 95% (17). Specificity did not change in either study.

Multi-plane reconstruction made from data collected by volume in a 3D sequence caused the obtained images to be of lower quality than the images from the output data. The images from reconstruction contained more distortion, artefacts, and sometimes higher noise than the original images.

In the presented study, after obtaining images in planes parallel to the CCL course, the authors determined the angles of inclination of the cross-section planes on the frontal image (angle α) and transverse image (angle β). The measurement made on images from 3D sequences was to determine the inaccuracy of line routing during geometric planning. The angle values α and β differed from zero, and their medians were 0.8° and 1.36°, respectively. The median angle α for the oblique sagittal plane was 7.76°, the median angle α was 6.53° for the double oblique sagittal plane, and the median angle β was 9.22°. The values of the angles differed considerably. The values of angles α were similar to those used by Böttcher *et al.* (5) assuming 5° and 10°, respectively. No information was found in the available literature on the effect of a double-oblique cross-sectional plane on CCL imaging in dogs, so it was impossible to compare the value of the angle β with the results of other studies.

The spatial determination of the imaging plane during MPR planning was performed by one operator, who subjectively assessed the improvement of CCL visibility on the basis of a real-time view of the obtained cross-section. During the study, a negative correlation ($P < 0.05$) was observed between the angles of the imaging plane and the assessment of CCL visibility and the number of images in which it can be seen. Increasing the value of angle α

(oblique sagittal plane) and angles α and β (double-oblique sagittal) significantly deteriorated CCL visibility. In another test determining the relationship between the values of these angles and weight, it was noticed that as the dog's weight increased, these angles decreased significantly (with reference to the double-oblique sagittal plane – 3D MPR DT). In interpretation of this, the authors suspect that the person performing the reconstruction tended to tilt the imaging plane more heavily for dogs with a lower weight, the images of which were of lower quality. In addition, the observed difference in the significance of the relationship between the dog's weight and angle α for the oblique sagittal plane ($P > 0.05$, median angle α 7.76°, interquartile range 7.22°) and that between the dog's weight and angle α for the double-oblique plane ($P < 0.05$, median angle α 6.53°, interquartile range 3.51°) may have resulted from the order in which oblique imaging planes were performed. When determining the slope of double-skewed planes, the plane affecting angle β was first determined, then that affecting angle α. The authors speculate that after determining the first plane and achieving an improvement in CCL visibility (on the preview), the second plane was tilted more carefully, i.e., by a smaller angle.

The study supports the final conclusion that imaging of the knee joint using 3D sequences makes possible the composition of higher quality images and better and more accurate visualisation of the cranial cruciate ligament. The research results have determined that multi-plane reconstruction affords an opportunity for the secondary determination of the oblique imaging planes and assembles images of equal quality to those of the 2D sequence and allows better visibility of the cranial cruciate ligament than 2D or 3D sequences. The study determined that the use of 3D and MPR sequences during magnetic resonance imaging visualises the cranial cruciate ligament precisely and repeatably.

References

1. A Ai T., Zhang W., Priddy N.K., Li X.: Diagnostic performance of CUBE MRI sequences of the knee compared with conventional MRI. Clin Radiol 2012, 67, e58–e63, doi: 10.1016/j.crad. 2012.07.020.
2. Banfield C.M., Morrison W.B.: Magnetic resonance arthrography of the canine stifle joint technique and applications in eleven

military dogs. Vet Radiol Ultrasound 2000, 41, 200–213, doi: 10.1111/j.1740-8261.2000.tb01479.x.

3. Barberie J.E., Carson B.W., Finnegan M., Wong A.D.: Oblique sagittal view of the anterior cruciate ligament: comparison of coronal vs. axial planes as localizing sequences. J Magn Reson Imaging 2001, 14, 203–206, doi: 10.1002/jmri.1174.

4. Blond L., Thrall D.E., Roe S.C., Chailleux N., Robertson I.D.: Diagnostic accuracy of magnetic resonance imaging for meniscal tears in dogs affected with naturally occuring cranial cruciate ligament rupture. Vet Radiol Ultrasound 2008, 49, 425–431, doi: 10.1111/j.1740-8261.2008.00401.x.

5. Böttcher P., Armbrust L., Blond L., Brühschwein A., Gavin P.R., Gielen I., Hecht S., Jurina K., Kneissl S., Konar M., Pujol E., Robinson A., Schaefer S.L., Theyse L.F., Wigger A., Ludewig E.: Effects of observer on the diagnostic accuracy of low-field MRI for detecting canine meniscal tears. Vet Radiol Ultrasound 2012, 53, 628–635, doi: 10.1111/j.1740-8261.2012.01967.x.

6. Breitenseher M.J., Mayerhoefer M.E.: Oblique MR imaging of the anterior cruciate ligament based on three-dimensional orientation. J Magn Reson Imaging 2007, 26, 794–798, doi: 10.1002/jmri.20922.

7. Buckwalter K.A., Pennes D.R.: Anterior cruciate ligament: oblique sagittal MR imaging. Radiology 1990, 175, 276–277, doi: 10.1148/radiology.175.1.2315495.

8. D'Anjou M.A., Moreau M., Troncy E., Martel-Pelletier J., Abram F., Raynauld J.P., Pelletier J.P.: Osteophytosis, subchondral bone sclerosis, joint effusion and soft tissue thickening in canine experimental stifle osteoarthritis: comparison between 1.5 T magnetic resonance imaging and computed radiography. Vet Surg 2008, 37, 166–177, doi: 10.1111/j.1532-950X.2007.00363.x.

9. Duc S.R., Pfirrmann C.W., Koch P.P., Zanetti M., Hodler J.: Internal knee derangement assessed with 3-minute three-dimensional isovoxel true FISP MR sequence: preliminary study. Radiology 2008, 246, 526–535, doi: 10.1148/radiol.2462062092.

10. Fazio C.G., Muir P., Schaefer S.L., Waller III K.R.: Accuracy of 3 Tesla magnetic resonance imaging using detection of fiber loss and a visual analog scale for diagnosing partial and complete cranial cruciate ligament ruptures in dogs. Vet Radiol Ultrasound 2018, 59, 64–78, doi: 10.1111/vru.12567.

11. Feichtenschlager C., Gerwing M., Failing K., Peppler C., Kása A., Kramer M., von Pückler K.H.: Magnetic Resonance Imaging Assessment of Intra-Articular Structures in the Canine Stifle Joint after Implantation of a Titanium Tibial Plateau Levelling Osteotomy Plate. Vet Comp Orthop Traumatol 2018, 31, 261–272, doi: 10.1055/s-0038-1647248.

12. Franklin S.P., Cook J.L., Cook C.R., Shaikh L.S., Clarke K.M., Holmes S.P.: Comparison of ultrasonography and magnetic resonance imaging to arthroscopy for diagnosing medial meniscal lesions in dogs with cranial cruciate ligament deficiency. J Am Vet Med Assoc 2017, 251, 71–79, doi: 10.2460/javma.251.1.71.

13. Galindo-Zamora V., Dziallas P., Ludwig D.C., Nolte I., Wefstaedt P.: Diagnostic accuracy of a short-duration 3 Tesla magnetic resonance protocol for diagnosing stifle joint lesions in dogs with non-traumatic cranial cruciate ligament rupture. BMC Vet Res 2013, 9, 40, doi: 10.1186/1746-6148-9-40.

14. Gokalp G., Demirag B., Nas O.F., Aydemir M.F., Yazici Z.: Contribution of thin slice (1 mm) oblique coronal proton density-weighted MR images for assessment of anteromedial and posterolateral bundle damage in anterior cruciate ligament injuries. Eur J Radiol 2012, 81, 2358–2365, doi: 10.1016/j.ejrad.2011.09.008.

15. Harper T.A., Jones J.C., Saunders G.K., Daniel G.B., Leroith T., Rossmeissl E.: Sensitivity of low-field T2* images for detecting the presence and severity of histopathologic meniscal lesions in dogs. Vet Radiol Ultrasound 2011, 52, 428–435, doi: 10.1111/j.1740-8261.2011.01818.x.

16. Jung J.Y., Jee W.H., Park M.Y., Lee S.Y., Kim J.M.: Meniscal tear configurations: categorization with 3D isotropic turbo spin-echo MRI compared with conventional MRI at 3 T. AJR Am J Roentgenol 2012, 198, W173–W180, doi: 10.2214/AJR.11.6979.

17. Kamal H.A., Abdelwahab N., El-Liethy N.E.: The role of oblique axial MR imaging in the diagnosis of ACL bundle lesions. Egypt J Radiol Nucl Med 2015, 46, 683–693, doi: 10.1016/j.ejrnm.2015.05.007.

18. Kijowski R., Davis K.W., Woods M.A., Lindstrom M.J., De Smet A.A., Gold G.E., Busse R.F.: Knee joint: comprehensive assessment with 3D isotropic resolution fast spin-echo MR imaging - diagnostic performance compared with that of conventional MR imaging at 3.0 T. Radiology 2009, 252, 486–495, doi: 10.1148/radiol.2523090028.

19. Kim S.I., Park H.J., Lee S.Y., Chung E.C., Kwon H.J., Cha J.G., Kim S.: Usefulness of oblique coronal and sagittal MR images of the knee after double-bundle and selective anterior cruciate ligament reconstructions. Acta Radiol 2015, 56, 312–321, doi: 10.1177/0284185114525952.

20. Kwon J.W., Yoon Y.C., Kim Y.N., Ahn J.H., Choe B.K.: Which oblique plane is more helpful in diagnosing an anterior cruciate ligament tear? Clin Radiol 2009, 64, 291–297, doi: 10.1016/j.crad.2008.10.007.

21. Lee J.E., Park H.J., Lee S.Y., Ahn J.H., Park J.H., Park J.Y.: Evaluation of selective bundle injury to the anterior cruciate ligament: T2-weighted fast spin-echo 3-T MRI with reformatted 3D oblique isotropic (VISTA) versus 2D technique. AJR Am J Roentgenol 2017, 209, W308–W316, doi: 10.2214/AJR.16.17659.

22. Likert R.: A technique for the measurement of attitudes. Arch Psychol 1932, 22, 55.

23. Martig S., Konar M., Schmökel H.G., Rytz U., Spreng D., Scheidegger J., Höhl B., Kircher P.R., Boisclair J., Lang J.: Low-field MRI and arthroscopy of meniscal lesions in ten dogs with experimentally induced cranial cruciate ligament insufficiency. Vet Radiol Ultrasound 2006, 47, 515–522, doi: 10.1111/j.1740-8261.2006.00179.x.

24. Matsui A., Shimizu M., Beale B., Takahashi F., Yamaguchi S.: Assessment of T2 relaxation times for normal canine knee articular cartilage by T2 mapping using 1.5-T magnetic resonance imaging. Vet Comp Orthop Traumatol 2017, 30, 391–397, doi: 10.3415/VCOT-17-01-0014.

25. Nakanishi K., Horibe S., Shiozaki Y., Ishida T., Narumi Y., Ikezoe J., Nakamura H.: MRI of normal anterior cruciate ligament (ACL) and reconstructed ACL: comparison of when the knee is extended with when the knee is flexed. Eur Radiol 1997, 7, 1020–1024, doi: 10.1007/s003300050244.

26. Nemec S.F., Marlovits S., Trattnig S., Matzek W., Mayerhoefer M.E., Krestan C.R.: High-resolution magnetic resonance imaging and conventional magnetic resonance imaging on a standard field-strength magnetic resonance system compared to arthroscopy in patients with suspected meniscal tears. Acad Radiol 2008, 15, 928–933, doi: 10.1016/j.acra.2008.02.007.

27. Nenezić D., Kocijancic I.: The value of the sagittal-oblique MRI technique for injuries of the anterior cruciate ligament in the knee. Radiol Oncol 2013, 47, 19–25, doi: 10.2478/raon-2013-0006.

28. Ng A.W.H., Griffith J.F., Hung E.H., Law K.Y., Yung P.S.: MRI diagnosis of ACL bundle tears: value of oblique axial imaging. Skeletal Radiol 2013, 42, 209–217, doi: 10.1007/s00256-012-1372-y.

29. Ng A.W.H., Griffith J.F., Law K.Y., Ting J.W., Tipoe G.L., Ahuja A.T., Chan K.M.: Oblique axial MR imaging of the normal anterior cruciate ligament bundles. Skeletal Radiol 2011, 40, 1587–1594, doi: 10.1007/s00256-011-1208-1.

30. Notohamiprodjo M., Horng A., Pietschmann M.F., Müller P.E., Horger W., Park J., Crispin A., Garcia del Olmo J.R., Weckbach S., Herrmann K.A., Reiser M.F., Glaser C.: MRI of the knee at 3T: first clinical results with an isotropic PDfs-weighted 3D-TSE-sequence. Invest Radiol 2009, 44, 585–597, doi: 10.1097/RLI.0b013e3181b4c1a1.

31. Ohishi T., Takahashi M., Abe M., Tsuchikawa T., Mori M., Nagano A.: The use of axial reconstructed images from three-dimensional MRI datasets for morphological diagnosis of meniscal tears of the knee. Arch Orthop Trauma Surg 2005, 125, 622–627, doi: 10.1007/s00402-004-0792-0.

32. Olive J., d'Anjou M.A., Cabassu J., Chailleux N., Blond L.: Fast presurgical magnetic resonance imaging of meniscal tears and concurrent subchondral bone marrow lesions: study of dogs with naturally occurring cranial cruciate ligament rupture. Vet Comp Orthop Traumatol 2014, 27, 1–7, doi: 10.3415/VCOT-13-04-0054.

33. Park H.J., Kim S.S., Lee S.Y., Park N.H., Ahn J.H., Chung E.C., Park J.Y., Kim M.-S.: Comparison between arthroscopic findings and 1.5-T and 3-T MRI of oblique coronal and sagittal planes of the knee for evaluation of selective bundle injury of the anterior cruciate ligament. AJR Am J Roentgenol 2014, 203, W199–W206, doi: 10.2214/AJR.13.11571.

34. Park H.J., Lee S.Y., Park N.H., Ahn J.H., Chung E.C., Kim S.J., Cha J.G.: Three-dimensional isotropic T2-weighted fast spin-echo (VISTA) knee MRI at 3.0 T in the evaluation of the anterior cruciate ligament injury with additional views: comparison with two-dimensional fast spin-echo T2-weighted sequences. Acta Radiol 2016, 57, 1372–1379, doi: 10.1177/0284185114568048.

35. Pass B., Robinson P., Hodgson R., Grainger A.J.: Can a single isotropic 3D fast spin echo sequence replace three-plane standard proton density fat-saturated knee MRI at 1.5 T? Br J Radiol 2015, 88, 20150189, doi: 10.1259/bjr.20150189.

36. Podadera J., Gavin P., Saveraid T., Hall E., Chau J., Makara M.: Effects of stifle flexion angle and scan plane on visibility of the normal canine cranial cruciate ligament using low-field magnetic resonance imaging. Vet Radiol Ultrasound 2014, 55, 407–413, doi: 10.1111/vru.12142.

37. Pujol E., Van Bree H., Cauzinille L., Poncet C., Gielen I., Bouvy B.: Anatomic study of the canine stifle using low-field magnetic resonance imaging (MRI) and MRI arthrography. Vet Surg 2011, 40, 395–401, doi: 10.1111/j.1532-950X.2011.00823.x.

38. Racette M., Al Saleh H., Waller III K.R., Bleedorn J.A., McCabe R.P., Vanderby Jr R., Markel M.D., Brounts S.H., Block W.F., Muir P.: 3D FSE Cube and VIPR-aTR 3.0 Tesla magnetic resonance imaging predicts canine cranial cruciate ligament structural properties. Vet J 2016, 209, 150–155, doi: 10.1016/j.tvjl.2015.10.055.

39. Ristow O., Steinbach L., Sabo G., Krug R., Huber M., Rauscher I., Ma B., Link T.M.: Isotropic 3D fast spin-echo imaging versus standard 2D imaging at 3.0 T of the knee – image quality and diagnostic performance. Eur Radio 2009, 19, 1263–1272, doi: 10.1007/s00330-008-1260-y.

40. Ruoff C.M., Eichelberger B.M., Pool R.R., Griffin IV J.F., Cummings K.J., Pozzi A., Padua A., Saunders W.B.: The use of small field-of-view 3 Tesla magnetic resonance imaging for identification of articular cartilage defects in the canine stifle: an ex vivo cadaveric study. Vet Radiol Ultrasound 2016, 57, 601–610, doi: 10.1111/vru.12420.

41. Sample S.J., Racette M.A., Hans E.C., Volstad N.J., Holzman G., Bleedorn J.A., Schaefer S.L., Waller III K.R., Hao Z., Block W.F., Muir P.: Radiographic and magnetic resonance imaging predicts severity of cruciate ligament fiber damage and synovitis in dogs with cranial cruciate ligament rupture. PloS One, 2017, 12, e0178086, doi: 10.1371/journal.pone.0178086.

42. Shigue D.A., Rahal S.C., Schimming B.C., Santos R.R., Vulcano L.C., Linardi J.L., Teixeira C.R.: Evaluation of the Marsh Deer Stifle Joint by Imaging Studies and Gross Anatomy. Anat Histol Embryol 2015, 44, 468–474, doi: 10.1111/ahe.12162.

43. Simpler R.E., Kerwin S.C., Eichelberger B.M., Wall C.R., Thompson J.A., Padua A., Purdy D., Griffin IV J.F.: Evaluation of the WARP-turbo spin echo sequence for 3 Tesla magnetic resonance imaging of stifle joints in dogs with stainless steel tibial plateau leveling osteotomy implants. Vet Radiol Ultrasound 2014, 55, 414–419, doi: 10.1111/vru.12141.

44. Soler M., Murciano J., Latorre R., Belda E., Rodríguez M.J., Agut A.: Ultrasonographic, computed tomographic and magnetic resonance imaging anatomy of the normal canine stifle joint. Vet J 2007, 174, 351–361, doi: 10.1016/j.tvjl.2006.08.019.

45. Spriet M., Mai W., McKnight A.: Asymmetric signal intensity in normal collateral ligaments of the distal interphalangeal joint in horses with a low-field MRI system due to the magic angle effect. Vet Radiol Ultrasound 2007, 48, 95–100, doi: 10.1111/j.1740-8261.2007.00211.x.

46. Winegardner K.R., Scrivani P.V., Krotscheck U., Todhunter R.J.: Magnetic resonance imaging of subarticular bone marrow lesions in dogs with stifle lameness. Vet Radiol Ultrasound 2007, 48, 312–317, doi: 10.1111/j.1740-8261.2007.00248.x.

47. Yoon Y.C., Kim S.S., Chung H.W., Choe B.K., Ahn J.H.: Diagnostic efficacy in knee MRI comparing conventional technique and multiplanar reconstruction with one-millimeter FSE PDW images. Acta Radiol 2007, 48, 869–874, doi: 10.1080/02841850701459791.